Journal of Physics: Conference Series **519** (2014) 012012 doi:10.1088/1742-6596/519/1/012012

A new chiral phase of $BiFeO_3$ evidenced from resonant x-ray Bragg diffraction.

A Rodriguez-Fernandez[1], S W Lovesey[2, 3], S P Collins[3], G Nisbet[3] and J A Blanco[1]

[1] Physics Department, University of Oviedo, C/ Calvo Sotelo s/n Oviedo, Spain
[2] ISIS Facility, STFC Oxfordshire OX11 0QX, UK
[3] Diamond Light Source Ltd, Oxfordshire OX11 0DE, UK

E-mail: angelrf86@gmail.com

Abstract. Results that support a new chiral phase in the only multiferroic material known above room temperature have been obtained by a resonant x-ray Bragg diffraction experiment, with the incoming x-ray beam tuned near the Fe K-edge (7.1135 keV), performed in its ferroelectric phase. The R3c forbidden reflection $(0,0,9)_H$ was studied as a function of the rotation of the crystal about the Bragg wavector in both phases, paramagnetic (700 K) and antiferromagnetic (300 K). The data gathered is consistent with a chiral structure formed by a circular cycloid propagating along $(1,1,0)_H$. Templeton and Templeton (T&T) scattering at 700 K is attributed in part to charge-like quadrupoles absent in a standard model of a cycloid in which a material vector generates all electronic states of the resonant ion. Extensive sets of azimuthal-angle data are used to infer values of three atomic multipoles in a satisfactory minimal model of the iron electronic structure, with a quadrupole (E1-E1 event) and a hexadecapole (E2-E2 event) contributing T&T scattering, plus a magnetic dipole (E1-E1).

1. Introduction

A rich variety of electronic phenomena have been revealed using scattering of x-rays at, or near, an absorption edge. These phenomena are of fundamental interest for the understanding of materials with unusual physical properties, such as $GaFeO_3$ [1], α-Fe_2O_3 [2] or the well-known Mott gap compound, V_2O_3 [3]. This technique has contributed towards the understanding of the multiferroic properties of $BiFeO_3$, the only compound known to support coupling between ferromagnetic and ferroelectric behaviours at room temperature. A better understanding of the physics that gives these material such interesting properties will help in the design of new multiferroic materials. [4]

Recently, multiferroic materials have been studied by many groups, due to the potential application for electronic devices such as sensors or multi-state memory storage-units. Of particular interest are materials that exhibit magnetoelectric properties [4-6], as is the case of the Bismuth Ferrite, $BiFeO_3$. Magnetoelectricity results from a cross-correlation of the magnetic and electric degrees of freedom of this kind of materials. This feature appears promising not only for spintronics but also for magnonics that use magnetic excitations for information processing. These materials support "spin waves" that can transport spin and hence information over macroscopic distances, without accompanying transport of charge, allowing direct control of the spin wave propagation without external magnetic fields [7].

The experimental technique used, Resonant Elastic X-ray Scattering, has advantages in the study of materials that show electronic magnetism and is able to obtain important information from the electronic properties (charge, spin and orbital degrees of freedom) of the materials, related to the angular anisotropy in the valence states, that is unobtainable by other neutron and X-ray probes [8,9]. In the case of intensities collected at space-group forbidden reflections we can access directly information about complex electronic structure which is manifest in atomic multipoles, including, magnetic charge, electric dipole, anapole, quadrupole, octupole and hexadecapole moments [2,3,10,11,12,13].

The following sections of this contribution are devoted to the discussion of the theory that is used to model a chiral long period ordering in materials belonging to the R3c space group family and presenting the Dzyaloshinky-Moriya interaction. Section 2 presents this model while Section 3 is devoted to the application of this description to a compound that displays this behaviour, $BiFeO_3$. The finally remarks are included in Section 4.

2. Theory

Bismuth Ferrite (Fig. 1) is a member of the R3c space group family, with Fe ions at 6a (Wyckoff position) sites. The symmetry related to these sites does not allow intensity by an electric dipole-electric dipole (E1-E1) event in the case of forbidden reflections of the type $(0,0,l)_H$ with l odd. However, diffraction enhanced by an electric quadrupole-electric quadrupole (E2-E2) events are allowed and can be produced by an atomic electric, time-even, hexadecapole.

Parity even multipoles are defined by the spherical tensors T^K_Q, where the positive integer K is the rank and Q the projection, with $-K \leq Q \leq K$. We represent the time average ‹...› by using angular brackets such as $\langle T^K_Q \rangle$, with a complex conjugate $\langle T^K_Q \rangle^* = (-1)^Q \langle T^K_{-Q} \rangle$. These multipoles are properties of the electronic ground-state, and the time-signature of this tensors $\langle T^K_Q \rangle$ is $(-1)^K$ [8,9]. The R3c space group symmetry allows the real part of the hexadecapole $\langle T^4_{+3} \rangle$. For the Fe ions in sites 6a in R3c structure, diffraction with wavevector $(0,0,l)_H$ is described by an electronic structure factor,

$$\Psi^K_Q = 3\left[\langle T^K_Q \rangle_1 + (-1)^l \langle T^K_Q \rangle_2\right], \tag{1}$$

where the relation between sites 1 and 2 is given by a rotation about the diagonal $\mathbf{a}_h + \mathbf{b}_h$ by 180° plus an inversion. Universal expressions for unit-cell structure factors are provided by Scagnoli and Lovesey [14]. Using (1) in an E2-E2 event, we obtain the following structure factor,

$$F_{\pi'\sigma} = \frac{3}{\sqrt{2}} \cos^3\theta \cos(3\psi) \mathrm{Re}\langle T^4_{+3} \rangle. \tag{2}$$

The contribution from the parity-odd E1-E2 events in the $\pi'\sigma$ channel of immediate interest comes from a purely real polar quadrupole, namely, $i(3/\sqrt{5}) \cos^2\theta \langle U^2_0 \rangle$ that is added to the hexadecapole contribution (2).

The presence of long range ordering due to a circular cycloid structure is responsible for a breaking of the symmetry inside the material. This motif related to the Dzyalosinky-Moriya interaction has been showed in many multiferroic materials as presented in the work by Przeniosło et al; see Model 1 in Figure 1 [15].

In the case of $BiFeO_3$, this break of symmetry could allow charge-like quadrupoles contribution (K=2) to be observed through an E1-E1 event. While electric dipole (E1-E1) transitions are normally appreciably stronger than an electric quadrupole (E2-E2) event, in this case as the diffraction from the quadrupoles is restricted due to crystal symmetry [16] and are expected to be vastly reduced in intensity.

We have defined the circular cycloid following Scagnoli and Lovesey assuming a super-cell length L=(2n+1)a, where a is one of the lattice parameters and n an integer related to the number of cells[14]. The integer f measures the wavevector in units of the fraction (2p/a)(a/L)=2p/(L(2n+1)), while the turn angle is equal to 2p/(2n+1). Multipoles for the super-cell are denoted by $\langle C^K_Q \rangle$. General results include: (a) Multipoles are symmetric under rotation by 180° about the axis normal to the plane of the cycloid. (b) Using the identity $C_{2x}\langle C^K_Q \rangle = (-1)^f \langle C^K_Q \rangle$ one finds the relation $\langle C^K_{-Q} \rangle = (-1)^f (-1)^K \langle C^K_Q \rangle$. (c) For given f and K all $\langle C^K_Q \rangle$ are proportional to one another. Scaling coefficients are complex and depend on both the magnitude and sign of the projection Q. (c) $\langle C^K_Q \rangle$ does not depend on n. (d) $\langle C^K_Q \rangle$ is not Hermitian. (e) $\langle C^K_Q \rangle = 0$ for $K < f$. These cycloid multipoles are not subject to the symmetry operations for sites 6a in the R3c group. For a circular cycloid rotating in the x-z plane,

$$\langle C^2_{+1} \rangle = \frac{1}{4}\left[\langle T^2_{+1} + T^2_{-1} \rangle + i\langle T^2_{+2} - T^2_{-2} \rangle\right]. \tag{3}$$

A representation of the quadrupole, $\langle T^2 \rangle$, in terms of standard operators is available [17]. Note that C^2_{+1} is purely real. Magnetic diffraction by the cycloid should be created by a time-odd dipole,

$$\langle C^1_0 \rangle = \frac{1}{2}\left[\langle T^1_0 \rangle - i\langle T^1_{-1} - T^1_{+1} \rangle/\sqrt{2}\right]. \tag{4}$$

A dipole $\langle T^1 \rangle$ is known to be a linear combination of spin, orbital moment and a dipole that expresses magnetic anisotropy [18]. However, in the absence of final state spin-orbit interactions only the orbital moment contributes at the K-edge [19].

Unit-cell structure factors in units of Ψ^2_{+1} are,

$$F_{\sigma'\sigma} = -i\sin(2\psi),$$

$$F_{\pi'\sigma} = t\cos\theta\sin\psi + u\cos^3\theta\cos(3\psi) - i\sin\theta\cos(2\psi)$$

$$-v(\sin\theta - i\cos\theta\sin\psi),$$

$$F_{\sigma'\pi} = t\cos\theta\sin\psi + u\cos^3\theta\cos(3\psi) + i\sin\theta\cos(2\psi)$$

$$-v(\sin\theta + i\cos\theta\sin\psi),$$

$$F_{\pi'\pi} = -i\sin^2(\theta)\sin(2\psi) - i\,v\sin(2\theta)\cos(\psi), \quad (5)$$

where θ is the Bragg angle and ψ is the azimuthal angle. Incorporating the two types of T&T mechanisms, we arrive at a unit-cell structure factor (5) that contains a second charge-like quadrupole, namely, Ψ^2_{+2}/Ψ^2_{+1} = -it, where t is a purely real value in the case of an ideal cycloid. The contribution from the hexadecapole is defined by $u=3\mathrm{Re}\langle T^4_{+3}\rangle/(\Psi^2_{+1}\sqrt{2})$. The magnetic contribution to the structure factor is $v = \Psi^1_1/(2\Psi^2_{+1})$. Since t and v both relate to an E1-E1 event they are nothing more than ratios of the appropriate multipoles that we have discussed. On the other hand, u has to include a ratio of radial integrals for E2-E2 and E1-E1 events, namely, $[q\ \{R^2\}_{sd}]^2/[\{R\}_{sp}]^2$ where $\{R\}_{sp}$ and $\{R^2\}_{sd}$.

The chiral property of the model that we present in this communication can be confirmed by a predicted contribution to intensity induced by circular polarization in the primary beam; the intensity in question is an outcome of matching chirality (helicity) in electronic structure and photons used in diffraction. The relevant intensity can be expressed in terms of unit-cell structure factors [12, 13], and after inserting expressions in (5) we arrive at,

$$\mathrm{Im}[(F_{\sigma'\pi})^* F_{\sigma'\sigma} + (F_{\pi'\pi})^* F_{\pi'\sigma}] = 2\cos\theta\cos\psi\,(v\sin\theta - \cos\theta\sin\psi)$$

$$\times\,(t\cos\theta\sin\psi + u\cos^3\theta\cos(3\psi) - v\sin\theta) \quad (6)$$

Note that the expression (6) does not vanish for v = 0, so resonant reflections have circular polarization dependence above T_N.

3. Application, $BiFeO_3$

Bismuth ferrite ($BiFeO_3$) shows both ferroic phases above room temperature. Below its Curie Temperature, $T_c \approx 1100$ K, it shows a ferroelectric behaviour with a polarization of 100 μC/cm^2. The magnetic structure of the ferric ions (Fe^{3+}) is described as a G-type antiferromagnetic ordering below the Néel temperature, T_N = 640 K, that coexist with a long-period incommensurate cycloid modulation (≈ 620 Å) in the hexagonal plane. The propagation vector of the magnetic order is very small (k~0) and therefore it appears very close to structural Bragg reflections, as shown in Figure 1 [21,22]. The spiral propagates along the vector $(1,1,0)_H$ with the dipole moments rotate in the $(-1,1,0)_H$ plane, defined by the spontaneous electric polarization along $[0,0,1]_H$ and the propagation vector.

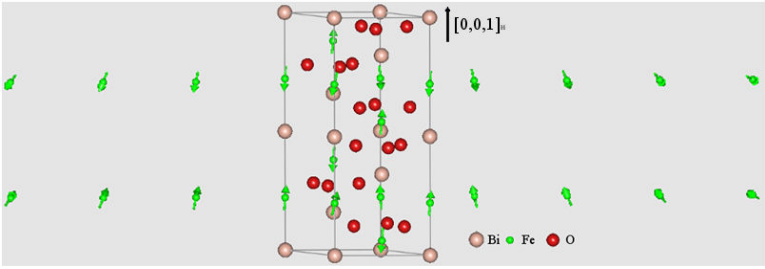

Figure 1. Scheme of the crystal and magnetic structures of bismuth ferrite ($BiFeO_3$), hexagonal $[0,0,1]_H$ axis is in the vertical. The arrows indicate the directions of Fe magnetic dipoles at room temperature.

The resonant x-ray experiments were performed at the Diamond Light Source (UK), with the synchrotron working at the energy of 3 GeV in the "top-up" mode. The beamline used was I16, equipped with a 6-circle kappa diffractometer and a focusing optical system that gives a photon flux on the sample position of 10^{13} photon/s and a beam size of 180×20 μm^2. The horizontally polarized beam, σ, delivered by a linear undulator was tuned near the Fe K-edge (7.1135 keV). As the high-quality single crystal used for the experiment (sizes 5 x 5mm^2 and a thickness of 0.5 mm) had a face perpendicular to the $(0,0,1)_H$ direction the experiment was performed with a specular geometry. While it is possible that the sample supports different domains, the very small size of the primary beam gives some confidence that a single domain is illuminated in our experiments. Indeed, we go on to show that, a chiral motif and a single domain are implied by our findings for the magnetically-ordered state.

The reflection studied was the forbidden $(0,0,9)_H$ in the space group #161. As is possible to observe from Figure 3 in ref (23), the weak contribution to the intensity by Bragg diffraction due to angular anisotropy is strongly enhanced by an atomic resonance. Two different studies were performed for the $(0,0,9)_H$ reflection at two different temperatures, below 300 K and above 700 K (the Néel Temperature). Following the scheme from Figure 2, all data collected were obtained in the rotated channel of polarization π'σ.

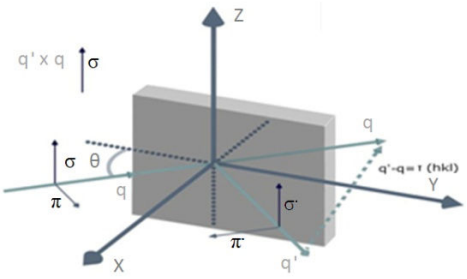

Figure 2. Scheme of the Cartesian coordinates (x, y, z) and x-ray polarization wavevectors. The plane of scattering defined by primary (**q**) and secondary (**q'**) wavevectors is parallel to the x-y plane. The components of the polarization labelled σ and σ' is normal to the plane and parallel to the z-axis, and polarization labelled π and π' lies in the plane of scattering.

The azimuthal scans presented in Figure 3 were obtained by performing "θ scans" with the detector around the Bragg condition for different azimuthal angles. This is one of the most common methods for performing azimuthal scans together with direct "ψ scans". Alternatively, one can measure the integrated intensity from a crystal analyzer, which may be pursued in the future. Coming back to the experimental method used in this experiment, the values displayed in Figure 3 are the integrated intensity of each of the curves normalized to the intensity of the primary x-ray beam. Due to the small penetration depth of an allowed Bragg spot $(0,0,6)_H$, where the diffraction strongly affacted by dynamical processes, we have not used this kind of reflection to normalize a forbidden Bragg spot $(0,0,9)_H$ that, due to its weakness has a kinematical behaviour, a larger penetration depth and is less affected by possible defects from the surface.

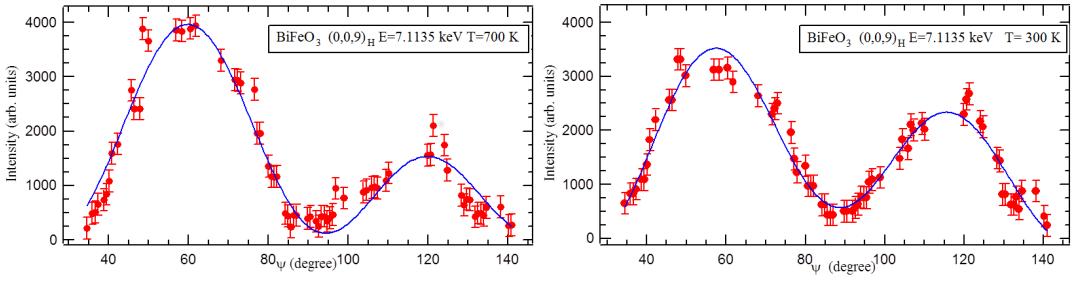

Figure 3. Templeton-Templeton scattering, at a reflection $(0,0,9)_H$ forbidden in R3c, as a function of azimuthal angle (red dots). (a) Shows data collected at the paramagnetic phase (700 K) while (b) present that of the antiferromagnetic phase (300 K). Solid line are a fit to our model of diffraction by a motif of charge-like quadrupoles and hexadecapoles, namely, $|F_{\pi'\sigma}|^2$ and expression (5) with v = 0 (v ≠ 0) for the paramagnetic (antiferromagnetic) case. Charge-like multipoles, t and u, are given the same values for both phases. Data taken from A. Rodriguez-Fernandez et al. [23]

One of the more complex steps in such kind of experiments is the extraction of the data coming directly from the intensity related to the angular anisotropy. Multiple scattering peaks, also known as Renninger reflections, were discriminated using a Matlab program available at the Beamline I16,

together with the selection of optimum positions by performing azimuthal scans in the case of the data obtained at room temperature, defining flat positions between peaks and avoiding the Renninger effect (therefore measured points in the azimuth dependence are not equidistant). Due to the fact that we have collected resonant x-ray data for a certain selected reflection at different parts of the single crystal, we consider that the experimental data shown in Figure 3 are related to the resonant event rather than to the tail of the Renninger effect.

Table 1. Values of the parameters used for the fitting for the two temperatures studied. In the case of 700K the parameter v was set to 0, see text for more details.

Parameter	700K	300K
t	1.19 ± 0.07	1.19 ± 0.07
u	- 6.20 ± 0.16	- 6.20 ± 0.16
v	-	0.673 ± 0.014

The Templeton-Templeton (T&T) scattering reported in Figure 3 taken from A Rodriguez et al. [23] shows the dependence at the two temperatures under study (3a) 700 K and (3b) 300 K ($T_N \approx 640$ K), both curves were obtained in the polarization channel $\pi'\sigma$ (Figure 2). From the data presented it can be observed that a possible E2-E2 event together with a contribution from the parity-odd E1-E2 resonance cannot explain the azimuthal dependence, these two contributions are in phase quadrature and they cannot interfere to break the pure six-fold periodicity that is lacking in Figure 3a (700 K).

We have simulated the Templeton-Templeton scattering using circular polarized light based on the values of refined multipoles from Table 1 obtained from the fitting to the experimental data (i.e., the values of all the multipoles therein, t, u and v). Figure 4 represents the different expected signal for scattering collected above and below the Néel temperature, $T_N \approx 640$ K. The theoretical dependences are adequately calculated by a model with minimal complexity. It includes Templeton and Templeton scattering [20] from charge-like quadrupoles and hexadecapoles. The contribution from quadrupoles is allowed because they participate in a chiral, circular cycloid, otherwise their contribution is forbidden in R3c. The chiral property of our model would be confirmed by a predicted contribution to intensity induced by circular polarization in the primary beam; the intensity in question is an outcome of matching chirality (helicity) in electronic structure and photons used in diffraction.

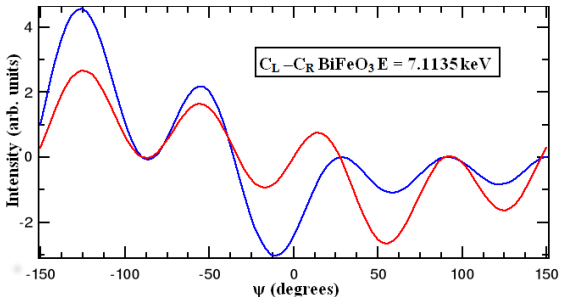

Figure 4. Simulation of the dichroic signal from Templeton-Templeton scattering under circular polarized x-rays for the reflection $(0,0,9)_H$ forbidden in R3c at the Fe K-edge. (Red line) Above and (blue line) below T_N (640K).

4. Conclusions

The study by X-ray resonant Bragg diffraction of the forbidden reflection $(009)_H$ for the R3c space group has revealed electronic properties of a single crystal of $BiFeO_3$. Existence of T&T scattering by quadrupoles in a cycloid implies a chemical structure that belongs to an enantiomorphic crystal class lacking a centre of symmetry. Space-group R3 (#146), one of 65 members of the Sohncke sub-group of crystal structures, is a maximal non-isomorphic subgroup of the nominal R3c-group, and thus a likely candidate for a commensurate chiral motif in bismuth ferrite. In this case, a chiral motif and a single domain are implied for the magnetically ordered state, and this does appear to be the case [25]. Quadrupoles (also higher-order multipoles) as a primary order-parameter is not unusual. However,

again, order is achieved at low temperatures, because the underlying mechanism is weak [26-28]. The origin of the charge-like quadrupoles that contribute to T&T scattering could be related to bismuth 6s-6p lone pairs, known to drive certain structural distortions. Apart from expected direct hybridization of lone pairs, there is scope for admixture through the agency of oxygen 2p states that contribute to angular anisotropy in valence states observed at iron sites.

Acknowledgements

We acknowledge the Diamond Light Source for the beamtime allocation on I16. One of us (SWL) is grateful to Dr D D Khalyavin and Dr K S Knight for valuable discussion about the explanation of results offered in the communication. We are also grateful with G Catalan, who has provided the single crystal for performing the experiment. Financial support has been received from Spanish FEDER-MiCiNN Grant No. Mat2011-27573-C04-02. One of us (ARF) is grateful to Gobierno del Principado de Asturias for the financial support from Plan de Ciencia, Tecnología e innovación (PTCI) de Asturias. We thank Diamond Light Source for access to beamline I16 (MT-7720) that contributed to the results presented here.

References

[1] Lovesey S W, Knight K S and Balcar E 2007 *J. Phys.: Condens. Matter* **19** 376205
[2] Lovesey S W, Rodriguez-Fernandez A, Blanco J A 2011 *Phys.Rev.B* **83** 054427
[3] Lovesey S W, Fernández Rodríguez J, Blanco J A, Sivia D S, Knight K S and Paolasini L 007 *Phys.Rev.B* **75** 014409
[4] Catalan G and Scott J F 2009 *Advance Materials* **21** 2463–2485
[5] Kadomtseva A M, Zvezdin A K, Popov Y F, Pyatakov A P and Vorob'ev G P 2004 *J. Exp. Theor. Phys. Lett.* **79** 571
[6] Scott J F 2010 *Adv. Mater.* **22** 2106
[7] Eerenstein, W 2006 Nature **422** 759
[8] Lovesey S W, Balcar E, Knight K S and Fernández-Rodriguez J 2005 *Phys. Rep.* **411** 233
[9] Lovesey S W and Balcar E 2013 *J. Phys. Soc. Japan* **82** 021008
[10] Lovesey S W and Scagnoli V 2009 *J. Phys.: Condens. Matter* **21** 474214
[11] Wilkins S B, Caciuffo R, Detlefs C, Rebizant J, Colineau E, Wastin F and Lander G H 2006 *Phys. Rev. B* **73** 060406
[12] Fernandez-Rodriguez J, Lovesey S W and Blanco J A 2008 *Phys. Rev. B* **77** 094441
[13] Rodriguez-Fernandez A, Lovesey S W, Scagnoli V, Staub U, Walker H C, Shukla D K, Strempfer J and Blanco J A 2013 *Phys.Rev.B* **88** 094437
[14] Scagnoli V and Lovesey S W 2009 *Phys. Rev. B* **79** 035111
[15] Przeniosło R, Regulski M and Sosnowska I 2006 *J. Phys. Soc. Japan* **75** 084718
[16] Hannon J P, Trammell G T, Blume M and Gibbs D 1988 *Phys. Rev. Lett.* **61** 1245; ibid 1989 **62** 2644 (E)
[17] Lovesey S W and Balcar E 1997 *J. Phys.-Condens. Matter* **9** 8679
[18] Carra P, Thole B T, Altarelli M and Wang X 1993 *Phys. Rev. Lett.* **70** 694
[19] Lovesey S W 1998 *J. Phys.: Condens. Matter* **10** 2505
[20] Palewicz A, Sosnowska I, Przeniosło R and Hewat A 2010 *Acta Physica Polonica* A **117** 296
[21] Lebeugle D, Colson D, Forget A, Viret M, Bataille A M and Gukasov A 2008 *Phys. Rev. Lett.* **100** 227602
[22] Lee S, Choi T, Ratcliff W, Erwin R, Cheong S W and Kiryukhin V 2008 *Phys. Rev. B* **78** 100101
[23] Rodriguez-Fernandez A, Lovesey S W, Collins S P, Nisbet G and Blanco J A 2014 *J. Phys. Soc. Japan* **83**, 013706
[24] Templeton D H and Templeton L K 1985 Acta Crystallogr. **41** 365; ibid 1986 **42** 478
[25] Johnson R D, Barone P, Bombardi A, Bean R J, Picozzi S, Radaelli P G, Oh Y S, Cheong S W and Chapon L C 2013 *Phys. Rev. Lett*. **110** 217206
[26] Morin P, Schmitt D and de Lacheisserie E 1982 *J. Magn. Magn. Mater.* **30** 257
[27] Sakakibara T, Tayama T, Onimaru T, Aoki D, Onuki Y, Sugawara H, Aoki Y and Sato H 2003 *J. Phys.: Condens. Matter* **15** S2055
[28] Kuramoto Y, Kusunose H and Kiss A 2009 *J. Phys. Soc. Japan* **78** 072001